

Identification of a prognostic immune signature for esophageal squamous cell carcinoma to predict survival and inflammatory landscapes

Jie He (✉ prof.jiehe@gmail.com)

National Cancer Center <https://orcid.org/0000-0002-0285-5403>

Chaoqi Zhang

National Cancer Center

Yuejun Luo

National Cancer Center

Zhen Zhang

The First Affiliated Hospital of Zhengzhou University

Zhihui Zhang

National Cancer Center

Guochao Zhang

National Cancer Center

Feng Wang

National Cancer Center

Yun Che

National Cancer Center

Yi Zhang

The First Affiliated Hospital of Zhengzhou University

Nan Sun

National Cancer Center

Research

Keywords: esophageal squamous cell carcinoma, immune signature, immune checkpoints, inflammatory landscape, individualized medicine

Posted Date: May 22nd, 2020

DOI: <https://doi.org/10.21203/rs.3.rs-29561/v1>

License:  This work is licensed under a Creative Commons Attribution 4.0 International License.

[Read Full License](#)

Abstract

Background

Immunotherapy has achieved surprising success in the treatment of esophageal squamous cell carcinoma (ESCC). However, studies concerning immune phenotypes within the ESCC microenvironment and their relationship with prognostic outcomes are limited. Therefore, we aim to construct and validate an individual immune-related risk signature for patients with ESCC.

Methods

We collected 196 ESCC cases, including 119 samples from our previous public data (GSE53624) to use as a training set. We additionally collected an independent validation cohort consisting of 77 frozen tumor tissues with qPCR data. Head and neck squamous cell carcinoma (HNSCC) and lung squamous cell carcinoma (LUSC) cohorts were also collected for validation. A least absolute shrinkage and selection operator (LASSO) model and a stepwise Cox proportional hazards regression model were used to construct the immune-specific signature. The potential mechanism and inflammatory landscapes of the signature were explored by using bioinformatics and immunofluorescence assay methods.

Results

Immune-related genes were significantly altered in ESCC tissues, and 16 differentially expressed immune-related genes with the most prognostic value were filtered out ($P<0.01$). Then a six-gene-based signature (*TSPAN2*, *AMBP*, *ITLN1*, *C6*, *PRLR*, and *MADCAM1*) was generated from the training set. This signature classified the patients into two groups with significantly different overall and relapse-free survival. Furthermore, the signature showed similar prognostic values in different clinical subgroups and in the independent cohort, as well as in patients with HNSCC and LUSC. Multivariable Cox regression analysis confirmed that the signature was an independent prognostic factor for patients with ESCC in different cohorts. Pathway analysis showed that genes related to the signature were mostly involved in cell adhesion, leukocyte transendothelial migration, and cancer progression. Further analysis revealed that the signature was closely associated with specific inflammatory activities (activation of macrophages and T cells signaling transduction). Additionally, high-risk patients were found characterized by distinctive immune checkpoints panel and higher filtration of Tregs and fibroblasts.

Conclusion

We constructed the first comprehensive immune-related risk signature for ESCC and furnished new hints of immune profiling of ESCC. Future prospective studies are needed to test the clinical utility of this signature in the individualized management of patients with ESCC.

Background

As reported by global cancer statistics in 2018, esophageal cancer (EC) is the sixth leading cause of cancer deaths, and the seventh most-common cancer worldwide [1], with an estimated 70% of EC cases occurring in China [2]. Esophageal cancer primarily includes two subtypes: esophageal squamous cell carcinoma (ESCC) and esophageal adenocarcinoma [3]. ESCC is the predominant histopathological type in China, and accounts for almost 90% of all EC cases [2]. Despite advancements in the standard treatment of EC, the prospect of enhancing the survival rate for such patients remains dismal [4], with an overall five-year survival rate that ranges from 15–25% [3, 5, 6]. Meanwhile, neoadjuvant chemoradiotherapy (nCRT) followed by resection has moderately improved the prognosis of patients with locally advanced ESCC compared to traditional surgery alone [7, 8]. For the moment, owing to high heterogeneity, patients with ESCC tend to exhibit individual differences in therapeutic efficacy, even under the same clinical-guidelines and recommended treatments. To some extent, this may attribute to the fact that clinical practices have failed to precisely stratify patients with ESCC, leading to the predicament of depersonalized, and often suboptimal treatment for each individual patient with ESCC. Therefore, there is an urgent and obligatory need to search for novel therapeutic strategies and stratification methods for patients with ESCC.

During past decades, immunotherapy, recognized as a milestone for cancer treatment, has advanced by leaps and bounds and revolutionized available treatment choices for several major cancer types[9, 10]. A clinical trial study of patients with advanced ESCC found that pembrolizumab (also known as "Keytruda"), acting as a second-line therapy, could remarkably improve overall survival (OS) compared with chemotherapy [11]. In 2019, the United States Food and Drug Administration (FDA) approved the use of pembrolizumab for the patients with advanced ESCC and high PD-L1 expression. Obviously, immunotherapy is increasing important to clinical practice and has emerged as a promising and potentially effective modality for treating ESCC. Several recent studies have focused on immune-related parameters to predict the survival of patients with EC, including some important immune molecules and cells. The results of these studies have further indicated the significance of the immune tumor microenvironment (TME)[12, 13]. Unfortunately, precision immunotherapy is hard to achieve without a comprehensive understanding of the landscape of the immune TME. However, there is still a scantiness of comprehensive analysis for the immune phenotype within the ESCC microenvironment and its relationship with prognosis and treatment outcomes.

Herein, we sought to establish and validate an immune-related risk signature for patients with ESCC. Firstly, we collected 196 ESCC cases from two independent cohorts consisting of GSE53624 and 77 frozen tumor tissues. Then, we constructed a risk signature by profiling an immune-related gene set with information extracting from the GSE53624 cohort. This signature was later validated in the independent cohort. Through these maneuvers, we built a practicable signature that is able to identify high-risk patients with ESCC. These patients generally exhibit worse survival than low-risk patients, both effectively and accurately. Such a signature will be useful for the clinical management and stratification of patients and will also help us understand the association between the ESCC immune TME and corresponding prognostic outcomes.

Methods And Material

Public mRNA data and samples collection

We used 196 ESCC cases in the present study, including 119 samples from our previously reported public data and 77 frozen surgically resected ESCC tissues from an independent cohort. Additionally, a total of 1011 LUSC and HNSC samples were downloaded from The Cancer Genome Atlas (TCGA) database (<https://cancergenome.nih.gov/>).

The correlative mRNA expression data and corresponding clinical information of 119 ESCC samples are publicly available (GSE53624) [14]. Also, we matched the unpublished recurrence-free survival (RFS) data with these 119 patients. The mRNA expression data of GSE53624 was firstly log2 transformed and quantile normalized, and the mean expression was regarded as the expression of genes with several probes. The 77 frozen tumor tissues collected from the First Affiliated Hospital of Zhengzhou University from 2011–2014. This research was approved by the Ethics Committee Board of the First Affiliated Hospital of Zhengzhou University.

Quantitative real-time polymerase chain reaction (qPCR) analysis

The qPCR analysis was carried out to assess the expression of immune-related genes in ESCC samples. Both RNA extraction and cDNA synthesis were based on the manufacturer's protocol. We employed a 10 μ l volume system, which includes 5 μ l SYBR Green Master Mix (Invitrogen), 3 μ l nuclease-free water, 1 μ l template, and 1 μ l of each PCR primer in the Agilent Mx3005P Real-Time PCR system. After that, all cDNA samples were diluted for qRT-PCR analysis. The expression values of six target genes were normalized to GAPDH, and then log2 transformed for the next analysis. The primer sequences of the six target genes and GAPDH used for qRT-PCR were displayed in Additional file 2: Table S1.

Immunofluorescence technique

ESCC tissues were fixed by using 10% neutral-buffered formalin and embedded in paraffin. Then the tissue sections (3 μ m) underwent deparaffinization and blocking for the next experiments. The PBS, including 2% BSA, was used to dilute the primary and secondary antibodies, which applied to stain α -SMA and Foxp3. Next, washing cells three times by PBS and staining the cell nuclei through 4, 6-diamidino-2-phenylindole (DAPI). The two independent experiments were performed.

Functional enrichment analysis

Gene ontology (GO) and Kyoto Encyclopedia of Genes and Genomes (KEGG) pathway analyses were carried out in DAVID 6.8 (<http://david.abcc.ncifcrf.gov/home.jsp>) and Cytoscape3.7.2. (<https://cytoscape.org/>).

xCell and Gene Set Variation Analysis(GSVA)

xCell (<http://xCell.ucsf.edu/>) is a novel tool to analyze the cellular heterogeneity landscape through gene profiles in bulk tumors includes almost 64 different immune and stromal cell types [15]. It was used to estimate the abundance of immune and stromal cell-type of each patient with ESCC. Also, the GSVA was performed with the GSVA package implemented in R-software version 3.5.1

Signature Generation and Statistical Analysis

A Univariate Cox proportional regression analysis was used to screen the immune-related genes notably associated with OS. Then, a least absolute shrinkage and selection operator (LASSO) model was performed to determine which prognostic genes, during this analysis, exhibited one standard error (SE) of the minimum criteria. Finally, taking into account the expression of selected genes and correlation estimated Cox regression coefficients, a risk score formula was generated for each patient. All patients were divided into high- and low-risk groups based on their risk scores. Overall survival of high- and low-risk patients was calculated using the Kaplan-Meier survival analysis method. The univariate and multivariate Cox proportional hazards regression model was performed to identify whether the risk score was an independent prognostic factor. All data analysis and generation of figures were achieved by R software version 3.5.1 (<https://www.r-project.org>) and SPSS 25.0 software. All statistical tests were two-sided. And a *P* value less than 0.05 was regarded as statistically significant.

Results

Immune-related profiles display significant differences between ESCC tissues and adjacent normal tissues

A total of 119 patients with ESCC with clinical data from GSE53624 were included as the training cohort, and the demographics of the cohort are listed in Additional file 2: TableS2. We downloaded 3104 immune-related genes from the AmiGO2 website, and finally, 2630 genes were matched in the GSE53624 training cohort. We analyzed the matched genes expression in ESCC tissues versus adjacent tissues. Among those immune-related genes, 513 were found to be differentially expressed in ESCC and adjacent tissues ($P<0.001$) (Fig.1A). GO analysis using Cytoscape 3.7.2 was performed to clarify the biological processes and pathways of these significant genes—which were mostly involved in the positive regulation of biological processes and leukocyte migration (e.g., intracellular signal transduction, cellular protein metabolic process, cell migration, and motility) (Fig.1B).

Construction of the immune-related prognostic signature

Firstly, the univariate Cox proportional regression analysis showed that 16 immune-related genes were statistically associated with OS ($P<0.01$) (Additional file 2: Table S3). We used the LASSO Cox regression model to filter the immune-related genes with the most prognostic value, and one SE of the minimum criteria was chosen. Eight genes were selected by this procedure, containing *TSPAN2*, *AMBP*, *ITLN1*, *C6*, *PRLR*, *RBM47*, *PLA2GS*, and *MADCAM1* (Figure 1C, 1D). Then, to optimize this model and reduce variables, a stepwise Cox proportional hazards regression analysis was performed. This method filtered out a six-gene (*TSPAN2*, *AMBP*, *ITLN1*, *C6*, *PRLR*, and *MADCAM1*) prognostic model.

We established a risk score model based on the expressions of these six genes, and corresponding coefficients for patients with ESCC, as follows: risk score = $(0.1272 \times TSPAN2 \text{ expression}) + (0.2423 \times AMBP \text{ expression}) + (0.2201 \times C6 \text{ expression}) + (0.1651 \times PRLR \text{ expression}) - (0.2720 \times ITLN1 \text{ expression}) - (0.2724 \times MADCAM1 \text{ expression})$. The risk score of every patient was calculated by this equation. All patients in the training cohort were classified into high- and low-risk groups according to the optimal cut-off point. Patients in the low-risk group had a longer OS than those in the high-risk group (HR 3.7144, 95% CI 2.2481–6.1370, $P<0.0001$) (Fig.2E). Similarly, low-risk patients also exhibited better RFS than high-risk ones (HR 2.2670, 95% CI 1.3142–3.9104, $P = 0.0026$) (Fig.2F). The time-dependent area under the ROC curves, demonstrating the predictive accuracy of this model, were 0.734, 0.783 and 0.802 in the GSE53624 set at 1, 3, and 5 years, respectively (Fig.2D). To further explore whether the risk score could serve as an independent prognostic factor for ESCC, univariate and multivariate Cox regression analyses were performed in the GSE53624 cohort. After incorporating some important clinical variables, such as age, sex, tobacco use, alcohol use, tumor location, tumor grade, T stage, N stage, and TNM stage, the risk score was still independently related to OS and RFS. (Table 1 &Additional file 2: TableS4)

Table 1
 Univariable and multivariable Cox regression analysis of the six-gene immune-related signature and overall survival in GSE53624 cohort.

Variable	Univariable analysis			Multivariable analysis		
	HR	95%CI	P value	HR	95%CI	P value
Age						
≥60 or <60	1.4206	0.8963-2.2516	0.1352			
Sex						
Male or female	1.2094	0.6846-2.1364	0.5126			
Smoking history						
Yes or no	0.8596	0.5322-1.3883	0.5361			
Alcohol history	1.0521	0.6559-1.6876	0.8333			
Yes or no						
Tumor location						
Upper, middle or lower	0.9610	0.5827-1.5851	0.8763			
Tumor grade						
Well, moderate or poor	1.2195	0.8550-1.7394	0.2733			
T stage						
1, 2, 3 or 4	1.1270	0.8387-1.5146	0.4277			
Lymphatic metastasis						
Yes or no	2.1594	1.3191-3.5350	0.0022	1.2331	0.5187-2.9317	0.6354
TNM stage						
I, II or III	1.9011	1.2262-2.9476	0.0041	1.2777	0.5372-3.0389	0.5794
Risk score						
High or low	3.7144	2.2481-6.1370	<0.0001	4.2511	2.4042-7.5166	<0.0001

Validation of the signature in stratified cohorts of ESCC

On account of the importance of lymph node metastasis in ESCC prognosis [16], we firstly investigated the relationship between OS and risk score for both lymph node metastasis positive (LN+) and lymph node metastasis negative (LN-) samples in the GSE53624 cohort. In both subgroups, low-risk patients exhibited significantly longer OS than high-risk ones (Additional file 1: Figure S1A, S1B). In the high-risk group, we also found that this signature suggested significantly poorer OS in the clinical feature subtypes of the training cohort, including early stage, advanced stage, older (age \geq 60), younger (age < 60), male, female, non-smoker, smoker, non-drinker, drinker(Additional file1: Figure S1-S2). It is evident that the prognostic performance of the six-gene signature was well validated when the training set was stratified by some important clinical features.

Validation of the signature in the independent cohort

To assess whether the six-gene signature could be applied in the clinical practice, we further validated in the independent cohort using qPCR analysis. The clinical characteristics of this validation cohort are shown in Additional file 2: TableS2. Risk scores of all patients were calculated using the same formula, and then assigned to high- and low-risk groups accordingly. This risk signature was well validated in the independent cohort. High-risk patients suffered unfavorable prognostic results in OS (HR 4.4096, 95% CI 1.6414–11.8465, $P = 0.0013$) and RFS (HR 4.7875, 95% CI 1.8440–12.4295, $P = 0.0004$) (Fig.3A–3E). In the same way, we detected the connection between OS and risk scores in the LN+ and LN- patients, respectively. In the LN+ subgroup, low-risk patients showed longer OS than their high-risk counterparts. However, this risk score showed a borderline difference between high- and low-risk patients in the LN- subgroup with a $P = 0.0540$ (Fig.3F,3G). We also used the same univariate and multivariate Cox regression model to analyze whether the risk score could also function as an independent predictor of prognosis in the independent cohort. As expected, we received the same conclusion as with the training cohort, the risk score was independently associated with OS and RFS (Table 2 and Additional file 2: TableS5).

Table 2
Univariable and multivariable Cox regression analysis of the six-gene

Variable	Univariable analysis			Multivariable analysis		
	HR	95%CI	P value	HR	95%CI	P value
Age						
≥60 or <60	2.2471	0.7655-6.5952	0.1406			
Sex						
Male or female	1.5951	0.5438-4.6793	0.3951			
Lymphatic metastasis						
Yes or no	5.3376	1.9912-14.3080	0.0009	2.9974	0.9399-9.5586	0.0636
TNM stage						
I, II or III	2.0551	1.2530-3.3709	0.0043	1.5058	0.7484-3.0298	0.2512
Risk score						
High or low	4.4097	1.6414-11.8465	0.0033	2.8332	1.0113-7.9372	0.0475

immune-related signature and overall survival in the independent validation cohort. Abbreviations: HR, hazard ratio; CI, confidence interval

Biological pathways analysis of the immune-related signature

We applied to GO analysis to determine the biological roles of this signature. The genes with Pearson $|R|>0.4$ were considered strongly linked to the risk score. We then generated a heatmap for these genes and the distribution of clinical features for every patient (Fig.4A). To identify fundamental biological functions, GO and KEGG analyses were carried out. Our results indicated that the risk score was related to several pathways, such as the cell adhesion, leukocyte transendothelial migration, and cancer progression, which may be associated with cancer metastasis (Fig.4B,4C). These findings may indicate that patients in the high-risk group are more likely to suffer lymphatic metastases.

Relationship between the risk score and immune landscapes

Owing to the establishment of the risk based on immune-related genes, we speculated that the risk might be relative to immune activities, immune response, and tumor microenvironment. Firstly, seven clusters of inflammatory and immune response genes (HCK, interferon, LCK, MHC-I, MHC-II, STAT1) were chosen and transformed to metagenes. As illustrated in Fig.5A, we found that most clusters are positively associated with the risk score, such as HCK and MHC II clusters. These seven clusters were subjected to the Gene Sets Variation Analysis (GSVA) to verify what we found in the seven metagene clusters. The results suggested that the high-risk score was mainly based upon genes related to the activation of macrophages and T cells signaling transduction (Fig.5C).

Immune checkpoints are extremely essential molecules in the immune TME. Therefore, we sought to examine the correlation between the risk score and immune checkpoints expression. We altogether enrolled 30 immune checkpoints in our analysis, including TNF superfamily (*BTLA*, *TNFSF14*, *CD40*, *TNFRSF4*, *TNFRSF9*, *CD27*, *CD40LG*, *TNFSF4*, *TNFSF9*, *CD70* and *TNFRSF18*) [17], B7-CD28 family (*CD274*, *PDCD1LG2*, *ICOSLG*, *CD276*, *VTCN1*, *HHLA2*, *CTLA4*, *ICOS*, *PDCD1*, and *TMIGD2*) [18, 19], and other immune checkpoint members (*HAVCR2*, *IDO1*, *LAG3*, *FGL1*, *ENTPD1*, *NT5E*, *SIGLEC15*, *C10orf54* and *NCR3*) [20–22]. The heatmap for immune checkpoints expression was produced, taking other clinical characteristics into consideration, such as sex, age, TNM stage, and lymphatic metastasis (Fig.5B). We observed that *TNFSF4*, *ICOSLG*, *PDCD1LG2*, *HAVCR2*, and *ENTPD1* were obviously upregulated in patients of the high-risk group. In contrast, *HHLA2*, *NCR3*, and *FGL1* were downregulated (Fig.5D, 5E). Most of these upregulated molecules are potential targets for cancer immunotherapy [23, 24]. This suggests that high-risk patients may benefit from the new immune targeted therapies.

Then, the xCell method was performed to investigate the TME cell infiltration. According to the analyzed result, high-risk groups exhibited increased infiltration of Tregs, CD4+ memory T cells, memory B cells, macrophages, several dendritic cells, and fibroblasts, and low infiltration of plasma cells, neutrophils, basophils, eosinophils (Fig.6A–6C). The previous research proved that Tregs could promote progression of ESCC, while both Tregs and fibroblasts were relevant to unfavorable survival in patients with ESCC [25–27]. Meanwhile, α-SMA and Foxp3 are specific biomarkers of fibroblasts and Treg cells [28, 29]. To confirm our analytical results, we firstly selected two presentative tumor samples from the high- and low-risk groups, and stained α-SMA and Foxp3 in the two tumor sample slices using the immunofluorescent assay method. The results, including Case 1 (a low-risk patient) and Case 2 (a high-risk patient), are shown in Fig.6D. These images verified that high-risk group patients demonstrate a higher infiltration of fibroblasts and Tregs.

Popularized the signature in the LUSC and HNSCC

ESCC resembled squamous carcinomas of other organs more than esophageal adenocarcinomas, especially LUSC and HNSC. Moreover, ESCC, LUSC, and HNSCC had familiar genetic backgrounds [30]. We collected 494 LUSC cases and 517 HNSCC samples from the TCGA database. The same risk score formula was applied to these two cohorts. Then, all patients were separated into high and low-risk groups

based on risk score. The patients with a high-risk score in the HNSCC cohort exhibited worse outcomes in OS (HR 1.6729, 95% CI 1.1297–2.2936, $P = 0.0012$) and RFS (HR 1.7928, 95% CI 1.1293–2.8463, $P = 0.0121$). For the LUSC cohort, patients in the high-risk group also suffered poorer prognosis in the OS (HR 1.5045, 95% CI 1.1407–21.9843, $P = 0.0036$); however, this risk score exhibited a borderline difference between high- and risk- group in RFS ($P = 0.0576$) (Fig.7). These results preliminarily proved that our signature had a favorable promotion value.

Discussion

Despite the combination of surgery, chemotherapy, and radiotherapy has been used to treat ESCC, patients with ESCC still suffer poor clinical outcomes. At the same time, immunotherapy has constantly demonstrated eye-catching and promising clinical results for ESCC, and is considered as a promising emerging treatment for ESCC [11]. Thus, it is essential to construct a useful and meaningful immune-related signature for ESCC. Such a signature could help us to assess the immune status of patients with ESCC. If it can be applied correctly, this immune-related signature will be a powerful prognostic biomarker for ESCC and enable us to stratify immunotherapeutic results. Up to now, there was a limited immune-related signature to predict prognosis in patients with ESCC. In our present research, we generated a six-gene-based immune-related signature through profiling an immune-related gene set, which exhibits a close connection with OS in patients with ESCC. This signature can effectively identify patients with ESCC at high risk for poor prognosis in the validation cohort. Meanwhile, the high-risk patients exhibited an enhanced local immune phenotype in contrast to their low-risk counterparts. This indicates that high-risk cases may benefit from immunotherapies.

Our prognostic signature was constructed using various immune-related genes containing protective (*ITLN1* and *MADCAM1*) and risky (*TSPAN2*, *AMBPs*, *C6*, and *PRLR*) genes. Regarding the two protective genes, *ITLN1*—also known as ometin-1—is a 34-KDa secretory protein and pleiotropic adipocytokine, possessing metabolic, inflammatory, and immune-related properties. *ITLN1* is highly expressed in the visceral adipose tissue, particularly in the stromal vascular cell [31]. *ITLN1* also carries prognostic value for various malignant tumors, such as colorectal, gastric cancers, and neuroblastoma. *ITLN1* was identified as a tumor suppressor in patients with gastric cancer and neuroblastoma. It is also related to improved survival in patients with gastric cancer [32, 33]. In patients with colorectal cancer, Kim et al. reported that *ITLN1* is a favorable prognostic biomarker in stage IV colorectal cancer [34]. In the contrary, a retrospective cohort research study revealed that there was a positive correlation between the level of circulating *ITLN1* concentrations and CRC risk [35]. *MADCAM-1*, a principal ligand of α4 integrins, is mainly expressed on endothelial cells and high endothelial venules of gut-associated lymphoid tissues, mediating the recruitment and activation of lymphocytes [36, 37]. Steiniger et al. specialized that fibroblasts expressing *MADCAM-1* that may attract CD4+T cells and instruct them into the periarteriolar T cell area [38]. However, there is no prognostic research of *ITLN1* and *MADCAM-1* in ESCC. Our findings suggest that *ITLN1* and *MADCAM1* are protective genes for ESCC. We believe more studies are needed to further illuminate the prognostic value of *ITLN1* and *CAMDAM-1* and their relevant mechanisms in patients with ESCC.

The roles of *TPSNA2*, *AMBP* and *PRLR* have not been confirmed in ESCC, but they were all found to be involved in the progression of various malignant cancers. For instance, *TPSNA2* performs a key function to suppress ROS production, leading to increased invasiveness and metastasis in lung and liver cancers. *TPSNA2* is also a poor outcome biomarker for patients with lung adenocarcinoma, and a protective gene for patients with acute myeloid leukemia [39, 40]. *AMBP* is an important member of the lipocalin superfamily, modulating the processes of inflammation [41]. Shoichi et al. pointed out that low expression of *AMBP* predicts an unfavorable prognosis in patients with oral squamous cell carcinoma [42]. *PRLP* acts as a vital receptor of PRL hormone., and after they get combined it will activate signals that suppress the epithelia-mesenchymal-transition processes and promote the invasiveness of breast cancer cells [43]. *PRLR* is an independent predictor of better outcomes in patients with breast cancer [44]. Conversely, it is a negative prognostic marker for patients with squamous cell carcinoma of the head and neck [45]. Finally, in our former study, *C6* was regarded as a risk-promoting factor in ESCC, in agreement with our present results [46].

We further investigated the relevant and possible mechanisms of the local immune risk signature. The genes related to the risk score were predominantly focused on cell adhesion, leukocyte transendothelial migration, and cancer progression pathways, which are related to cancer metastasis. The risk score was also positively associated with HCK and MCH metagenes. Thus, high-risk scores were based upon genes relevant to the activation of macrophages and T cell signaling transduction. High-risk patients exhibited higher expression of *TNFSF4*, *ICOSLG*, *PDCD1LG2*, *HAVCR2*and *ENTPD1*. These molecules are strongly associated with T cell activation and responses. For example, *TNFSF4*—also known as OX40L—is a ligand of OX40, and its combination withOX40 regulates T cell proliferation, activation, and survival, and even has an effect on cytokine release from T cells [47].*ICOS* signaling is an essential part of regulating Th1, Th2, and Th17 immunity [48].*ICOSLG*, a vital ligand of ICOS, also plays a crucial role in the regulation of T cell immunity [24]. *PDCD1LG2*, *HAVCR2*, and *ENTPD1* contribute to immune tolerance in the TME. These genes suppress the anti-tumor function of T cell [49–51]. These immune checkpoints may be potential and promising targets for cancer immunotherapy. These findings hold broad implications for patients with cancer. We also found higher infiltration of Tregs in high-risk patients.Tregs are well-known mediators that contribute to immunologic tolerance, weakening T cell activation, and responsiveness [52, 53]. All these findings remind us that high-risk cases are more likely to profit from immunotherapies. In the meantime, these results can help us to comprehend the real immune status of patients within different risk cohorts, which also may be conducive to clinical instruction.

We have constructed an initial immune-related signature to predict prognosis for patients with ESCC [46]; however, there were some limitations to the previous research. On the one hand, we enrolled approximately 708 immune-related genes, which may not be sufficient for a comprehensive analysis. On the other hand, our previous study lacked a qPCR validation to avoid the false-positive error of sequencing. The design of this study addressed these limitations to some degree. We enrolled 2630 immune-related genes in the present study, applied the robust risk score method, and further validated our findings in an independent cohort. However, our present study also has several limitations. This project lacked a large population cohort to make further validations. Additionally, this was retrospective research

and should be tested in prospective cohorts. Finally, the predictive capacity of our six-gene immune-related signature may not be sufficiently stable for the high spatial heterogeneity in the immune TME.

In conclusion, we established a more comprehensive immune-related risk signature for ESCC and furnished new information related to immune profiling of ESCC. The clinical value and application range of this signature cannot be ignored. We also believe our findings may assist clinicians decide on individual management and treatment strategies for patients with ESCC.

Abbreviations

AUC Area under the curve

CI Confidence interval

ESCC Esophageal squamous cell carcinoma

GO Gene Oncology

GVSA Gene Set Variation Analysis

HNSCC Head and neck squamous cell carcinoma

HR Hazard ratio

KEGG Kyoto Encyclopedia of Genes and Genomes

LUSC Lung squamous cell carcinoma

NA Not available

OS Overall survival

qPCR Quantitative real-time polymerase chain reaction

RFS Recurrence-free survival

ROC Receiver operating characteristic

TME Tumor environment

Declarations

Ethics approval and consent to participate

This research was approved by the Ethics Committee Board of the First Affiliated Hospital of Zhengzhou University.

Consent for publication

Not applicable.

Availability of data and materials

Most of the data sets used and/or analyzed during the current study are publicly available data from TCGA and Gene Expression Omnibus (GEO) databases (GSE63264). All data of the independent cohort in the current study were available from the corresponding authors in a reasonable request.

Competing interests

The authors declare that they have no competing interests.

Funding

This work was supported by the CAMS Innovation Fund for Medical Sciences (2017-I2M-1-005, 2016-I2M-1-001), the National Natural Science Foundation of China (81802299, 81502514), the Fundamental Research Funds for the Central Universities (3332018070), and the National Key Basic Research Development Plan (2018YFC1312105).

Authors' contributions

Jie He and Nan Sun designed the study. Chaoqi Zhang performed the analysis. Chaoqi Zhang and Yuejun Luo wrote the manuscript and contributed to the Immunofluorescence of clinical samples. Zhen Zhang and Yi Zhang performed the validation in the independent cohort. Zhihui Zhang, Guochao Zhang, and Feng Wang developed the inclusion criteria and normalized the expression profile data. Yun Che contributed to preparing the figures and tables. All authors reviewed the manuscript and approved the final version.

Acknowledgements

All authors would like to thank the specimen donors for this study and research groups for the LUSC and HNSCC samples from TCGA.

References

- 1.Bray F, Ferlay J, Soerjomataram I, Siegel RL, Torre LA, Jemal A: *Global cancer statistics 2018: GLOBOCAN estimates of incidence and mortality worldwide for 36 cancers in 185 countries*. CA Cancer J

- 2.Chen R, Zheng RS, Zhang SW, Zeng HM, Wang SM, Sun KX, Gu XY, Wei WW, He J: [Analysis of incidence and mortality of esophageal cancer in China, 2015]. *Zhonghua Yu Fang Yi Xue Za Zhi* 2019, 53:1094–1097.
- 3.Pennathur A, Gibson MK, Jobe BA, Luketich JD: *Oesophageal carcinoma*. *Lancet* 2013, 381:400–412.
- 4.Cohen DJ, Leichman L: *Controversies in the treatment of local and locally advanced gastric and esophageal cancers*. *J Clin Oncol* 2015, 33:1754–1759.
- 5.Chen W, Zheng R, Baade PD, Zhang S, Zeng H, Bray F, Jemal A, Yu XQ, He J: *Cancer statistics in China, 2015*. *CA Cancer J Clin* 2016, 66:115–132.
- 6.Huang FL, Yu SJ: *Esophageal cancer: Risk factors, genetic association, and treatment*. *Asian J Surg* 2018, 41:210–215.
- 7.Allum WH, Blazeby JM, Griffin SM, Cunningham D, Jankowski JA, Wong R: *Guidelines for the management of oesophageal and gastric cancer*. *Gut* 2011, 60:1449–1472.
- 8.Shapiro J, van Lanschot JJB, Hulshof M, van Hagen P, van Berge Henegouwen MI, Wijnhoven BPL, van Laarhoven HWM, Nieuwenhuijzen GAP, Hospers GAP, Bonenkamp JJ, et al: *Neoadjuvant chemoradiotherapy plus surgery versus surgery alone for oesophageal or junctional cancer (CROSS): long-term results of a randomised controlled trial*. *Lancet Oncol* 2015, 16:1090–1098.
- 9.Akinleye A, Rasool Z: *Immune checkpoint inhibitors of PD-L1 as cancer therapeutics*. *J Hematol Oncol* 2019, 12:92.
- 10.Liu T, Han C, Wang S, Fang P, Ma Z, Xu L, Yin R: *Cancer-associated fibroblasts: an emerging target of anti-cancer immunotherapy*. *J Hematol Oncol* 2019, 12:86.
- 11.Metges J, Francois E, Shah M, Adenis A, Enzinger P, Kojima T, Muro K, Bennouna J, Hsu C, Moriaki T, et al: *The phase 3 KEYNOTE-181 study: pembrolizumab versus chemotherapy as second-line therapy for advanced esophageal cancer*. *Ann Oncol* 2019, 30 Suppl 4:iv130.
- 12.Huang WT, Lu HI, Wang YM, Chen YH, Lo CM, Lin WC, Lan YC, Tseng LH, Li SH: *Positive Programmed Cell Death-Ligand 1 Expression Predicts Poor Treatment Outcomes in Esophageal Squamous Cell Carcinoma Patients Receiving Neoadjuvant Chemoradiotherapy*. *J Clin Med* 2019, 8.
- 13.Yagi T, Baba Y, Ishimoto T, Iwatsuki M, Miyamoto Y, Yoshida N, Watanabe M, Baba H: *PD-L1 Expression, Tumor-infiltrating Lymphocytes, and Clinical Outcome in Patients With Surgically Resected Esophageal Cancer*. *Ann Surg* 2019, 269:471–478.

- 14.Li J, Chen Z, Tian L, Zhou C, He MY, Gao Y, Wang S, Zhou F, Shi S, Feng X, et al: *LncRNA profile study reveals a three-lncRNA signature associated with the survival of patients with oesophageal squamous cell carcinoma*. Gut 2014, 63:1700–1710.
- 15.Aran D, Hu Z, Butte AJ: *xCell: digitally portraying the tissue cellular heterogeneity landscape*. Genome Biol 2017, 18:220.
- 16.Kakegawa T: *Forty years' experience in surgical treatment for esophageal cancer*. Int J Clin Oncol 2003, 8:277–288.
- 17.Ward-Kavanagh LK, Lin WW, Sedy JR, Ware CF: *The TNF Receptor Superfamily in Co-stimulating and Co-inhibitory Responses*. Immunity 2016, 44:1005–1019.
- 18.Janakiram M, Chinai JM, Zhao A, Sparano JA, Zang X: *HHLA2 and TMIGD2: new immunotherapeutic targets of the B7 and CD28 families*. Oncoimmunology 2015, 4:e1026534.
- 19.Zhang C, Zhang Z, Li F, Shen Z, Qiao Y, Li L, Liu S, Song M, Zhao X, Ren F, et al: *Large-scale analysis reveals the specific clinical and immune features of B7-H3 in glioma*. Oncoimmunology 2018, 7:e1461304.
- 20.Chretien S, Zerde I, Bergh J, Matikas A, Foukakis T: *Beyond PD-1/PD-L1 Inhibition: What the Future Holds for Breast Cancer Immunotherapy*. Cancers (Basel) 2019, 11.
- 21.Wang J, Sanmamed MF, Datar I, Su TT, Ji L, Sun J, Chen L, Chen Y, Zhu G, Yin W, et al: *Fibrinogen-like Protein 1 Is a Major Immune Inhibitory Ligand of LAG-3*. Cell 2019, 176:334–347.e312.
- 22.Wang J, Sun J, Liu LN, Flies DB, Nie X, Toki M, Zhang J, Song C, Zarr M, Zhou X, et al: *Siglec-15 as an immune suppressor and potential target for normalization cancer immunotherapy*. Nat Med 2019, 25:656–666.
- 23.Du W, Yang M, Turner A, Xu C, Ferris RL, Huang J, Kane LP, Lu B: *TIM-3 as a Target for Cancer Immunotherapy and Mechanisms of Action*. Int J Mol Sci 2017, 18.
- 24.Marinelli O, Nabissi M, Morelli MB, Torquati L, Amantini C, Santoni G: *ICOS-L as a Potential Therapeutic Target for Cancer Immunotherapy*. Curr Protein Pept Sci 2018, 19:1107–1113.
- 25.Fu L, Zhang C, Zhang LY, Dong SS, Lu LH, Chen J, Dai Y, Li Y, Kong KL, Kwong DL, Guan XY: *Wnt2 secreted by tumour fibroblasts promotes tumour progression in oesophageal cancer by activation of the Wnt/beta-catenin signalling pathway*. Gut 2011, 60:1635–1643.
- 26.Nabeki B, Ishigami S, Uchikado Y, Sasaki K, Kita Y, Okumura H, Arigami T, Kijima Y, Kurahara H, Maemura K, Natsugoe S: *Interleukin-32 expression and Treg infiltration in esophageal squamous cell carcinoma*. Anticancer Res 2015, 35:2941–2947.

- 27.Yue Y, Lian J, Wang T, Luo C, Yuan Y, Qin G, Zhang B, Zhang Y: *Interleukin-33-nuclear factor-kappaB-CCL2 signaling pathway promotes progression of esophageal squamous cell carcinoma by directing regulatory T cells*. *Cancer Sci* 2020, 111:795–806.
- 28.Korn T, Muschawechk A: *Stability and Maintenance of Foxp3(+) Treg Cells in Non-lymphoid Microenvironments*. *Front Immunol* 2019, 10:2634.
- 29.Zhan S, Liu Z, Zhang M, Guo T, Quan Q, Huang L, Guo L, Cao L, Zhang X: *Overexpression of B7-H3 in alpha-SMA-Positive Fibroblasts Is Associated With Cancer Progression and Survival in Gastric Adenocarcinomas*. *Front Oncol* 2019, 9:1466.
- 30.Lin DC, Dinh HQ, Xie JJ, Mayakonda A, Silva TC, Jiang YY, Ding LW, He JZ, Xu XE, Hao JJ, et al: *Identification of distinct mutational patterns and new driver genes in oesophageal squamous cell carcinomas and adenocarcinomas*. *Gut* 2018, 67:1769–1779.
- 31.Jaikanth C, Gurumurthy P, Cherian KM, Indhumathi T: *Emergence of omentin as a pleiotropic adipocytokine*. *Exp Clin Endocrinol Diabetes* 2013, 121:377–383.
- 32.Li D, Mei H, Pu J, Xiang X, Zhao X, Qu H, Huang K, Zheng L, Tong Q: *Intelectin 1 suppresses the growth, invasion and metastasis of neuroblastoma cells through up-regulation of N-myc downstream regulated gene 2*. *Mol Cancer* 2015, 14:47.
- 33.Li D, Zhao X, Xiao Y, Mei H, Pu J, Xiang X, Jiao W, Song H, Qu H, Huang K, et al: *Intelectin 1 suppresses tumor progression and is associated with improved survival in gastric cancer*. *Oncotarget* 2015, 6:16168–16182.
- 34.Kim HJ, Kang UB, Lee H, Jung JH, Lee ST, Yu MH, Kim H, Lee C: *Profiling of differentially expressed proteins in stage IV colorectal cancers with good and poor outcomes*. *J Proteomics* 2012, 75:2983–2997.
- 35.Aleksandrova K, di Giuseppe R, Isermann B, Biemann R, Schulze M, Wittenbecher C, Fritzsche A, Lehmann R, Menzel J, Weikert C, et al: *Circulating Omentin as a Novel Biomarker for Colorectal Cancer Risk: Data from the EPIC-Potsdam Cohort Study*. *Cancer Res* 2016, 76:3862–3871.
- 36.Rose DM, Han J, Ginsberg MH: *Alpha4 integrins and the immune response*. *Immunol Rev* 2002, 186:118–124.
- 37.Kuhbandner K, Hammer A, Haase S, Terbrack E, Hoffmann A, Schippers A, Wagner N, Hussain RZ, Miller-Little WA, Koh AY, et al: *MAdCAM-1-Mediated Intestinal Lymphocyte Homing Is Critical for the Development of Active Experimental Autoimmune Encephalomyelitis*. *Front Immunol* 2019, 10:903.
- 38.Steiniger B, Barth P, Hellinger A: *The perifollicular and marginal zones of the human splenic white pulp: do fibroblasts guide lymphocyte immigration?* *Am J Pathol* 2001, 159:501–512.

- 39.Lin SY, Miao YR, Hu FF, Hu H, Zhang Q, Li Q, Chen Z, Guo AY: *A 6-Membrane Protein Gene score for prognostic prediction of cytogenetically normal acute myeloid leukemia in multiple cohorts.* *J Cancer* 2020, 11:251–259.
- 40.Otsubo C, Otomo R, Miyazaki M, Matsushima-Hibiya Y, Kohno T, Iwakawa R, Takeshita F, Okayama H, Ichikawa H, Saya H, et al: *TSPAN2 is involved in cell invasion and motility during lung cancer progression.* *Cell Rep* 2014, 7:527–538.
- 41.Akerstrom B, Logdberg L, Berggard T, Osmark P, Lindqvist A: *alpha(1)-Microglobulin: a yellow-brown lipocalin.* *Biochim Biophys Acta* 2000, 1482:172–184.
- 42.Sekikawa S, Onda T, Miura N, Nomura T, Takano N, Shibahara T, Honda K: *Underexpression of alpha-1-microglobulin/bikunin precursor predicts a poor prognosis in oral squamous cell carcinoma.* *Int J Oncol* 2018, 53:2605–2614.
- 43.Nouhi Z, Chughtai N, Hartley S, Cocolakis E, Lebrun JJ, Ali S: *Defining the role of prolactin as an invasion suppressor hormone in breast cancer cells.* *Cancer Res* 2006, 66:1824–1832.
- 44.Hachim IY, Hachim MY, Lopez VM, Lebrun JJ, Ali S: *Prolactin Receptor Expression is an Independent Favorable Prognostic Marker in Human Breast Cancer.* *Appl Immunohistochem Mol Morphol* 2016, 24:238–245.
- 45.Bauernhofer T, Pichler M, Wieckowski E, Stanson J, Aigelsreiter A, Griesbacher A, Groselj-Strele A, Linecker A, Samonigg H, Langner C, Whiteside TL: *Prolactin receptor is a negative prognostic factor in patients with squamous cell carcinoma of the head and neck.* *Br J Cancer* 2011, 104:1641–1648.
- 46.Li Y, Lu Z, Che Y, Wang J, Sun S, Huang J, Mao S, Lei Y, Chen Z, He J: *Immune signature profiling identified predictive and prognostic factors for esophageal squamous cell carcinoma.* *Oncoimmunology* 2017, 6:e1356147.
- 47.Reuter D, Staeghe MS, Kuhnol CD, Foll J: *Immunostimulation by OX40 Ligand Transgenic Ewing Sarcoma Cells.* *Front Oncol* 2015, 5:242.
- 48.Wikenheiser DJ, Stumhofer JS: *ICOS Co-Stimulation: Friend or Foe?* *Front Immunol* 2016, 7:304.
- 49.Duhen T, Duhen R, Montler R, Moses J, Moudgil T, de Miranda NF, Goodall CP, Blair TC, Fox BA, McDermott JE, et al: *Co-expression of CD39 and CD103 identifies tumor-reactive CD8 T cells in human solid tumors.* *Nat Commun* 2018, 9:2724.
- 50.Rozali EN, Hato SV, Robinson BW, Lake RA, Lesterhuis WJ: *Programmed death ligand 2 in cancer-induced immune suppression.* *Clin Dev Immunol* 2012, 2012:656340.
- 51.Sabatos CA, Chakravarti S, Cha E, Schubart A, Sanchez-Fueyo A, Zheng XX, Coyle AJ, Strom TB, Freeman GJ, Kuchroo VK: *Interaction of Tim-3 and Tim-3 ligand regulates T helper type 1 responses*

and induction of peripheral tolerance. *Nat Immunol* 2003, 4:1102–1110.

52. Aykut B, Chen R, Miller G: Regulatory T Cells Keep Pancreatic Cancer at Bay. *Cancer Discov* 2020, 10:345–347.

53. Yang L, Li A, Lei Q, Zhang Y: Tumor-intrinsic signaling pathways: key roles in the regulation of the immunosuppressive tumor microenvironment. *J Hematol Oncol* 2019, 12:125.

Figures

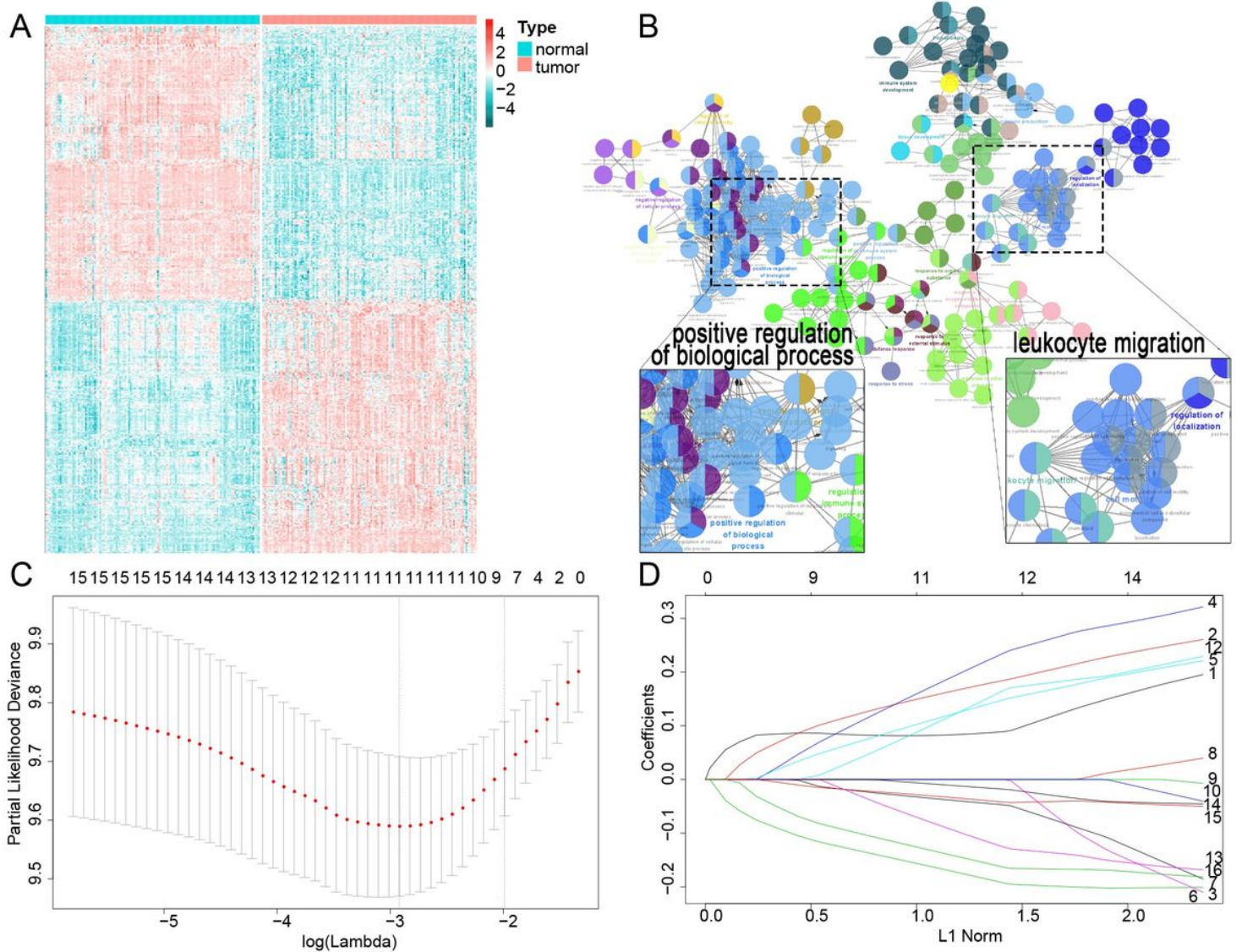


Figure 1

Filter out the most prognostic candidates from the differentially expressed immune-related genes in ESCC. (A) Heatmap of differentially expressed immune-related genes between ESCC and adjacent normal tissues. (B) GO analysis in Cytoscape of these differential genes. (C) 100-fold cross-validation for tuning

parameter selection in the LASSO model. (D) LASSO coefficient profiles of the most useful prognostic genes

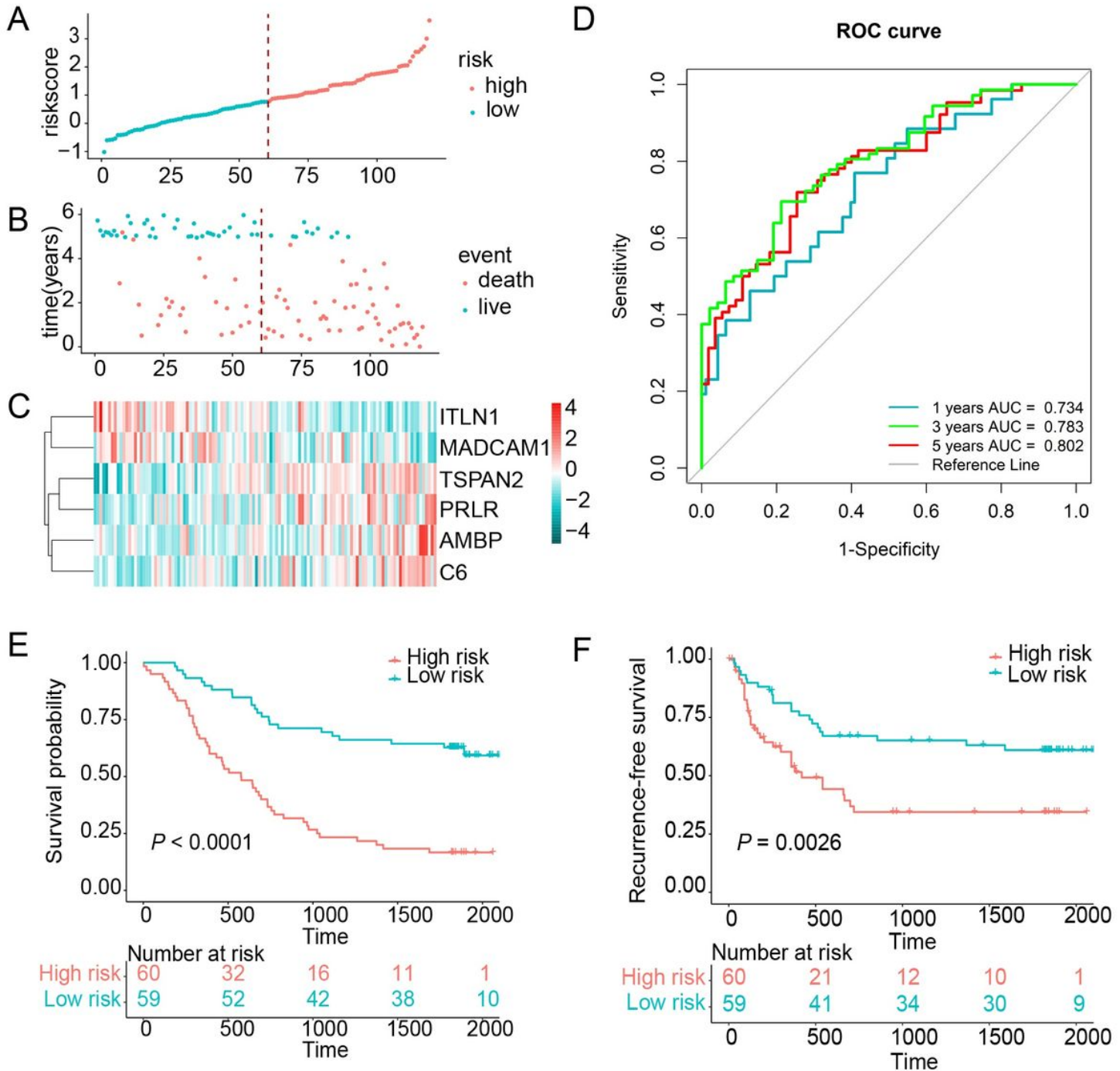


Figure 2

Risk score distribution and survival of patients in the training cohort. (A) The risk scores for 119 patients in the training cohort (GSE53624) are plotted in ascending order and marked as high risk (red) and low risk (green). (B) Survival of each patient in the cohort. Death is indicated by the color red, and alive patients are indicated by the color green. (C) Expression distribution of the six genes in the training cohort, with red indicating higher expression and blue indicating lower expression. (D) ROC analysis of immune

related genes signature for prediction of survival at 1, 3, and 5 years in the training cohort. (E&F) Kaplan-Meier curves of OS and RFS in 119 patients of the training cohort based on risk score, respectively

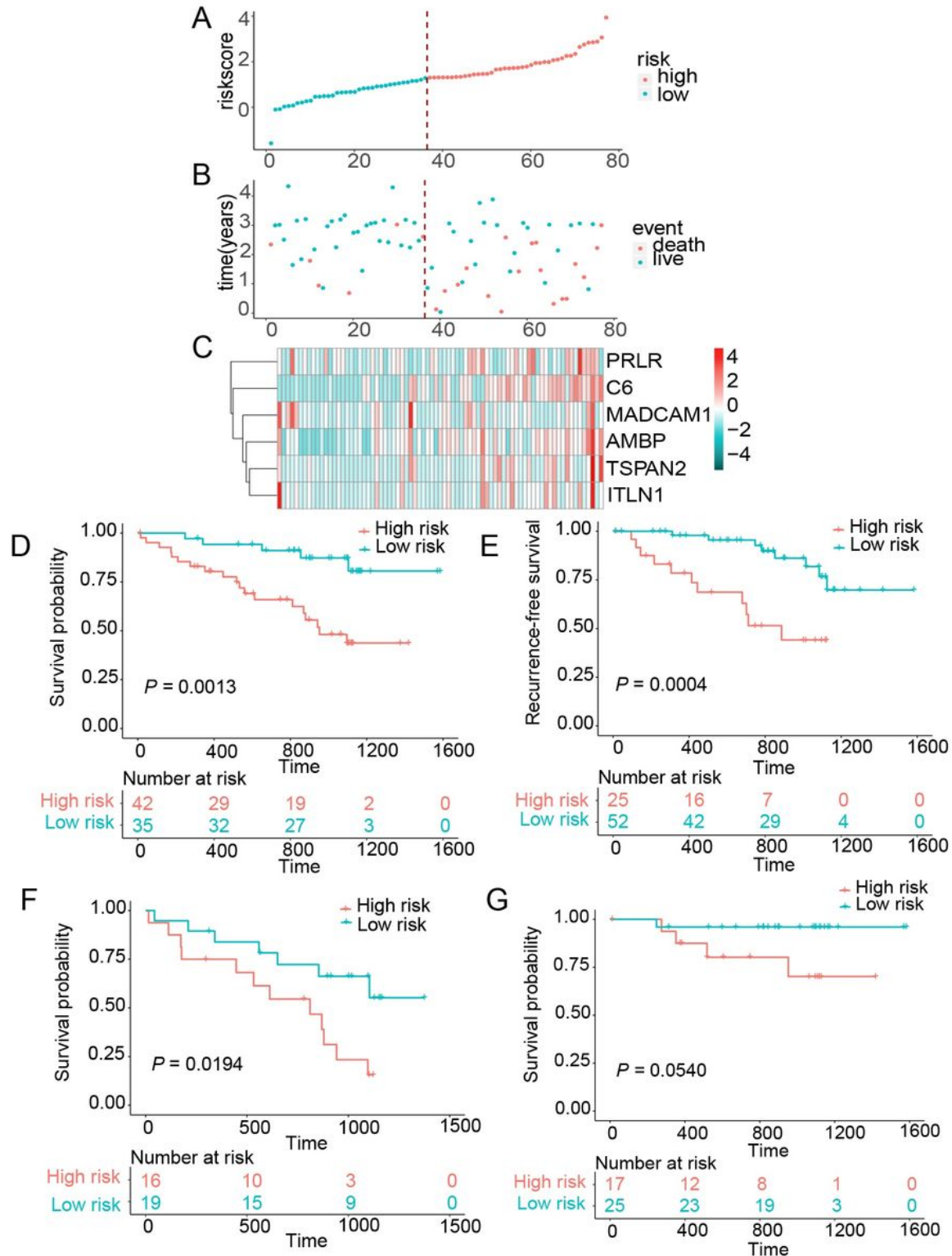
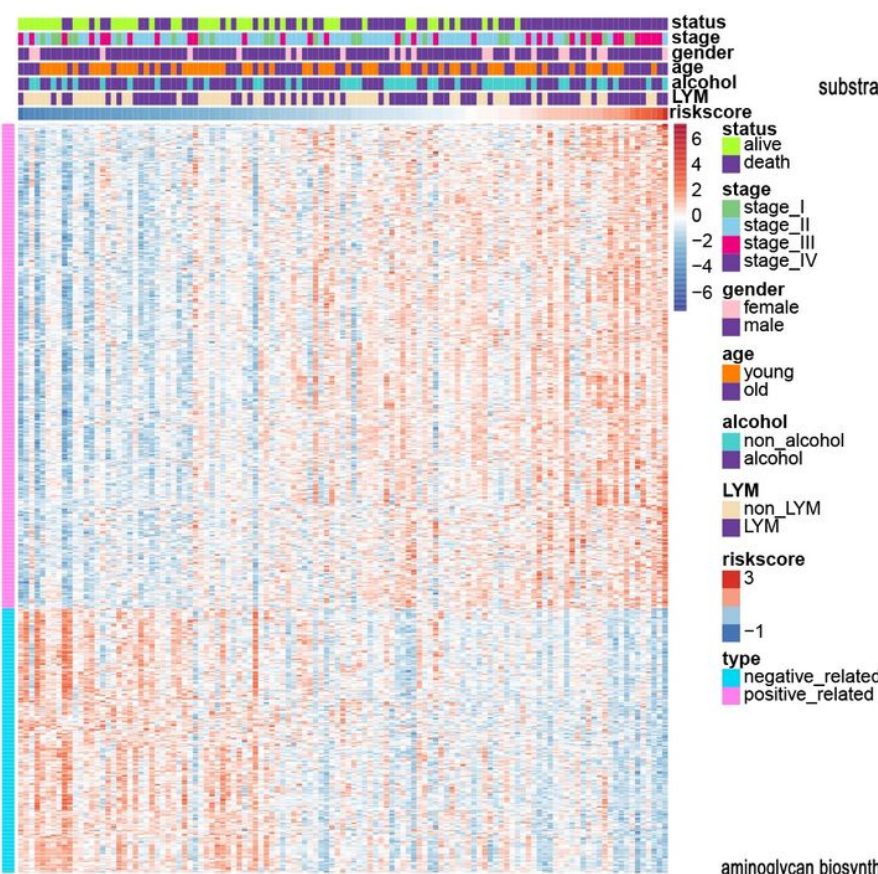


Figure 3

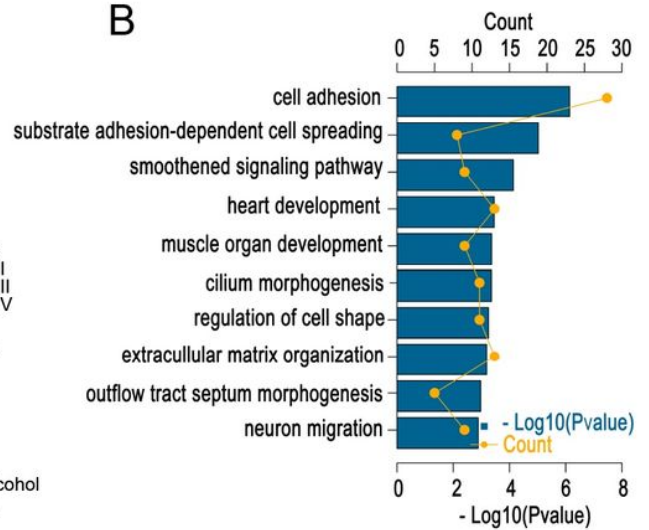
Risk score distribution and survival of patients in the clinical validation cohort. (A) The risk scores for 79 patients of the clinical validation cohort. (B) The survival of each patient in the clinical validation cohort. (C) Expression distribution of the six genes in the clinical validation cohort. (D&E) Kaplan-Meier curve of

OS and RFS in clinical validation cohort. (F&G) Kaplan-Meier curves of OS in LN+ and LN- patients of clinical validation cohort.

A



B



C

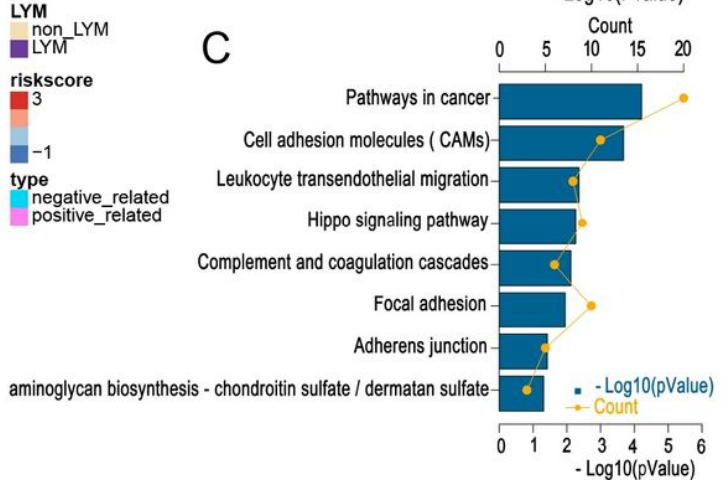


Figure 4

Relationship between risk score and most relevant immune-related genes and biological pathways. (A) Details of risk score and the most relevant genes. (B) Gene enrichment with Go terms of the selected genes. (C) Gene enrichment with KEGG terms of the selected genes

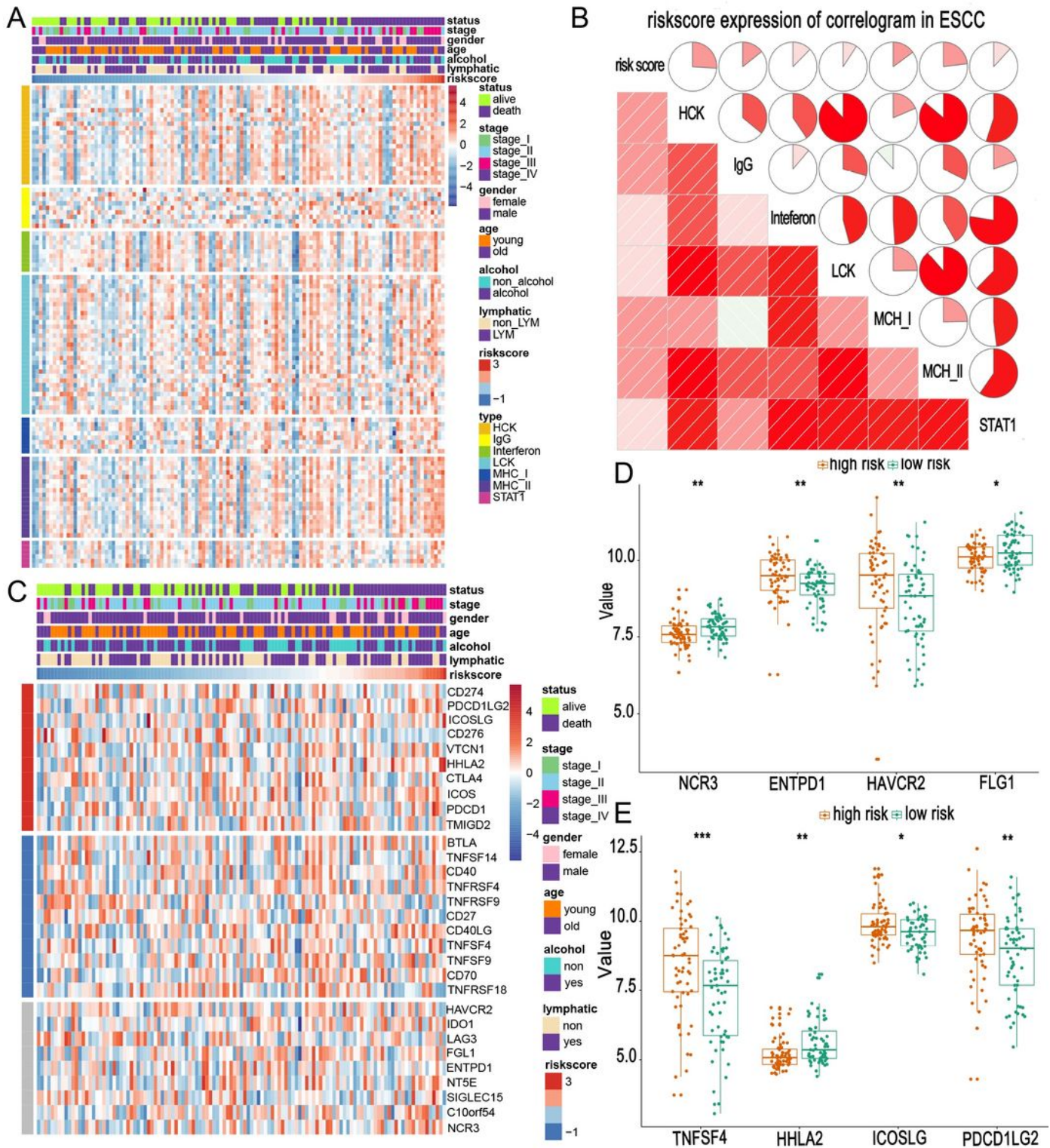
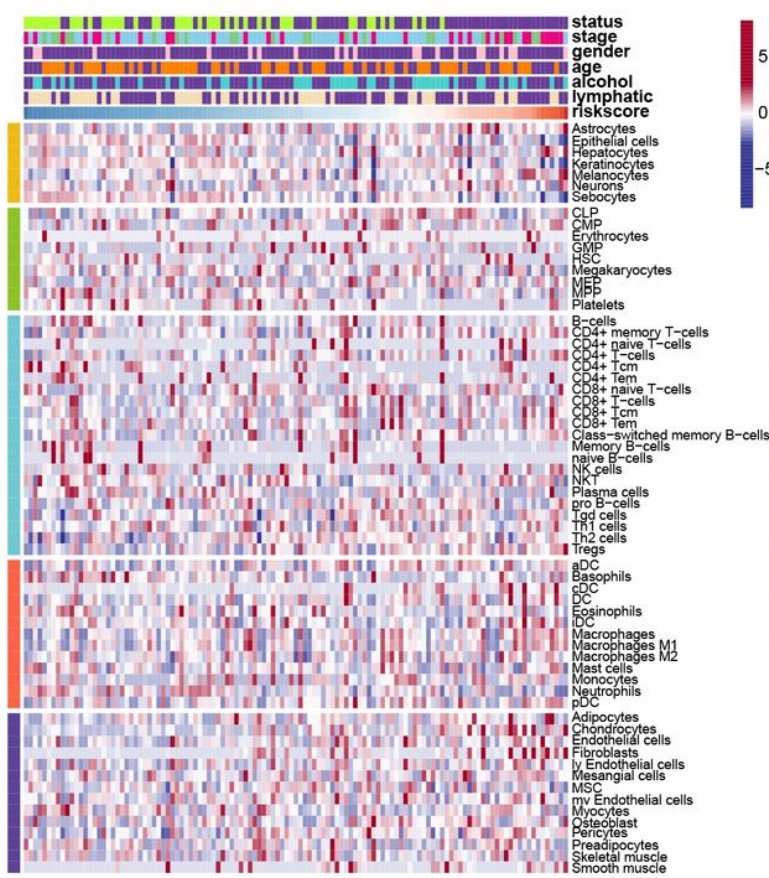


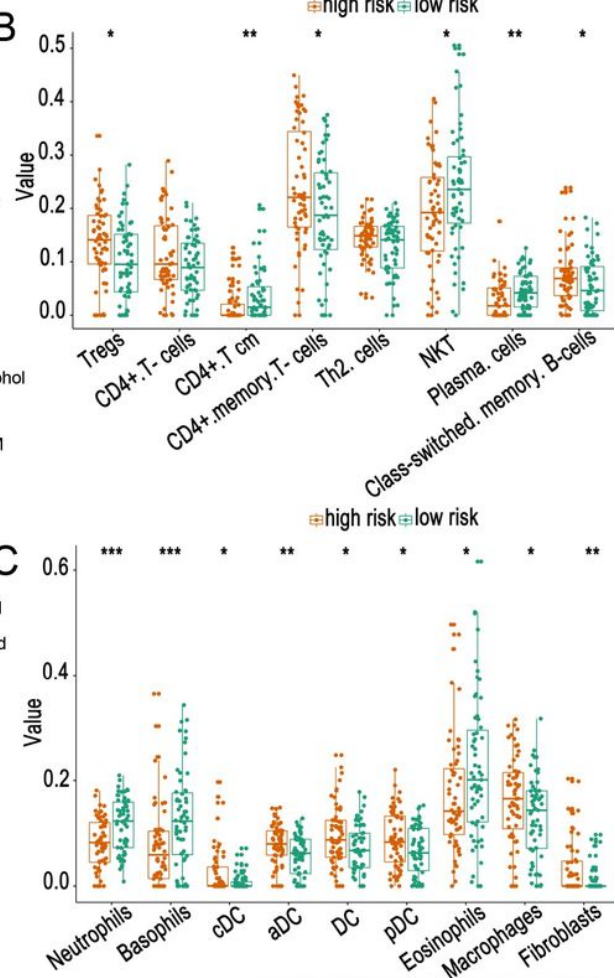
Figure 5

Relationship between risk scores and immune metagenes and immune checkpoints. (A&C) Expression of metagenes heatmap and correlogram in the training cohort. (B) The expression profile of immune checkpoints landscapes in the training cohort. (D&E) Different expression of immune checkpoints in high- and low-risk groups. *, **, and *** represent $P < 0.05$, $P < 0.01$, and $P < 0.001$, respectively

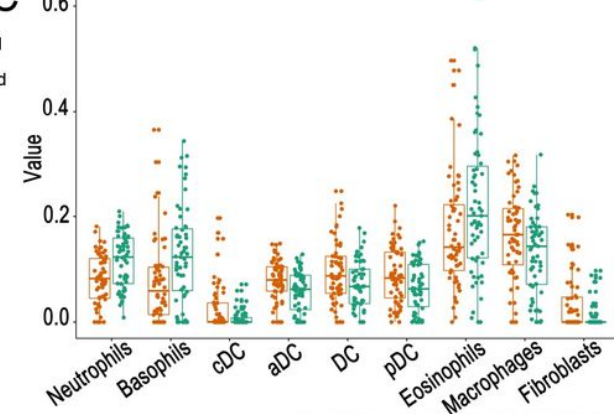
A



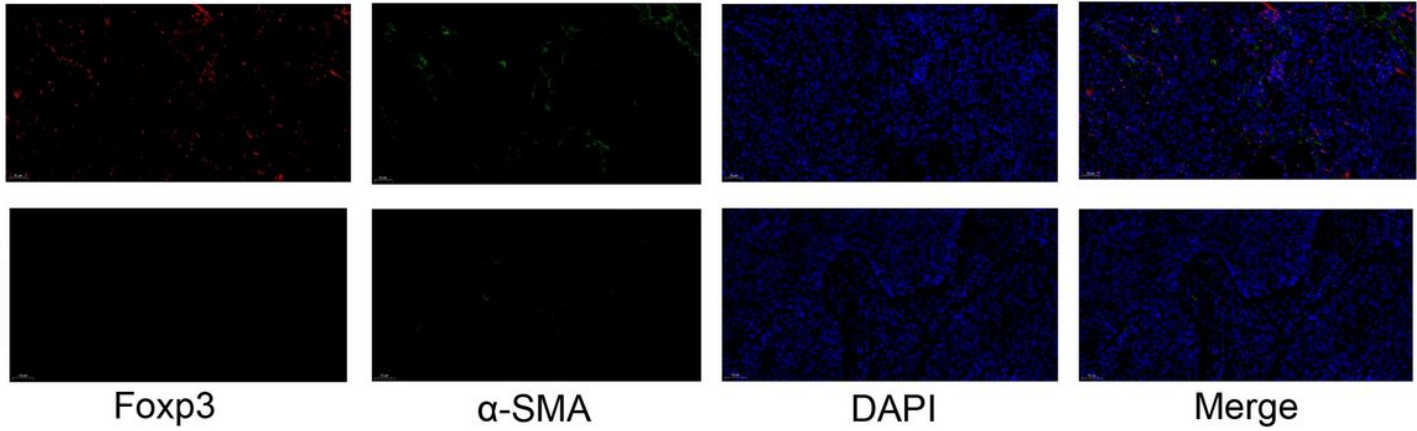
B



C



Case1



Foxp3

α-SMA

DAPI

Merge

Figure 6

Relationship between risk score and different cells estimated by xCell. (A) The landscape of risk score and different cell infiltration. (B&C) Different distribution of estimated cells in high- and low-risk groups. (D) Immunofluorescence images of Tregs and fibroblasts in tissues from the high-risk group (Case 1) and low-risk group (Case 2) respectively. The foxp3 is marked as red, and α-SMA is marked as green. (200X) *, **, and *** represent $P < 0.05$, $P < 0.01$, and $P < 0.001$, respectively

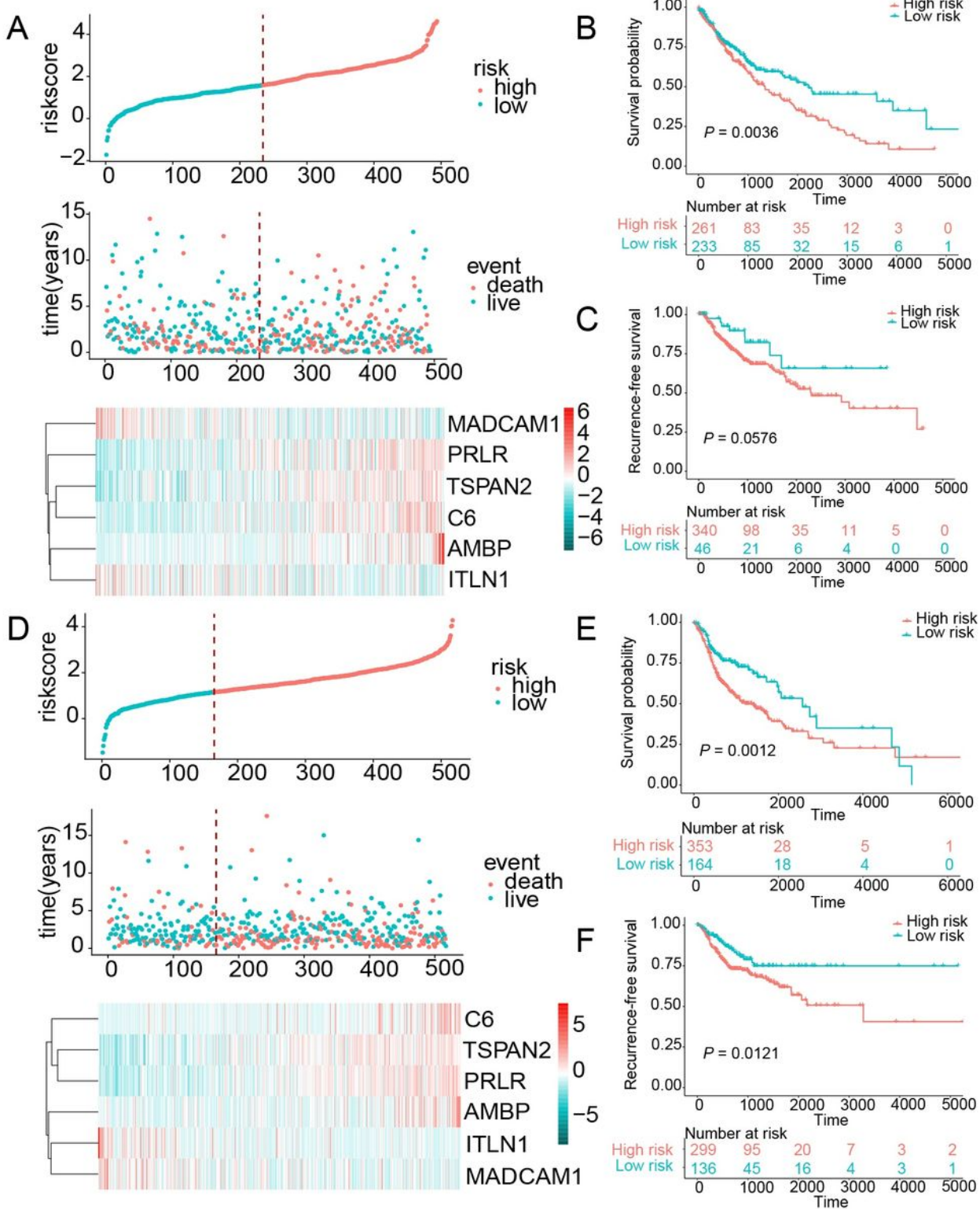


Figure 7

Risk score distribution and survival of patients in the LUSC and HNSCC cohorts. (A) The risk scores for 494 patients of the LUSC cohort, the survival of each patient, and gene expression distribution in the LUSC cohort. (B&C) Kaplan-Meier curve of OS and RFS in the LUSC cohort respectively. (D) The risk scores for 517 patients of the HNSCC cohort, the survival of each patient, and gene expression

distribution in the HNSCC cohort. (E&F) Kaplan-Meier curve of OS and RFS in the HNSCC cohort respectively

Supplementary Files

This is a list of supplementary files associated with this preprint. Click to download.

- [Additionalfile2.docx](#)
- [Additionalfile1.pdf](#)